
The influence of the vehicle's front-end profile upon adult pedestrian kinematics and dynamics, multibody approach

Adrian Soica* and Nicolae Ispas

Department of Vehicles and Transport Engineering,
Faculty of Mechanical Engineering,
Transilvania University of Brasov,
Bd. Eroilor, no.29, zip code 500036, Brasov, Romania
Email: a.soica@unitbv.ro
Email: inicu@unitbv.ro
*Corresponding author

Abstract: The research aims to simulate and compare with experimental data road traffic accidents involving adult pedestrians. The analysis focuses on the contact phase between the pedestrian and the vehicle's front end, using a multibody model. Taking into account the wide range of vehicles involved in such events as mentioned in the analyses from work of Depriester and Masson, the researchers aim to establish a correlation between the vehicle's front end and the pedestrian's kinematics and dynamics. By modifying certain frontal geometry parameters, various vehicle profiles were obtained in accordance with the classification from the Dettinger's study. The impact velocity and motor vehicle frontal structures, including geometry and rigidity, have proved to be important factors that produce trauma. In this paper, the vehicle's bumper assembly parameters were modified; and experimental researches and simulations were completed to determine the influence of the front-end vehicle design on the adult pedestrian kinematics and head dynamics.

Keywords: multibody; vehicle safety; pedestrian accident reconstruction; accident simulation.

Reference to this paper should be made as follows: Soica, A. and Ispas, N. (2012) 'The influence of the vehicle's front-end profile upon adult pedestrian kinematics and dynamics, multibody approach', *Int. J. Vehicle Safety*, Vol. 6, No. 2, pp.134–148.

1 Introduction

Each year, in the European Union, approximately 40,000 people die and another more than 1 million are injured in road traffic accidents. Almost 20% of these traffic-related fatalities involved either pedestrians (6000) or cyclists (2300) (Kalliske and Friesen, 2001). These statistics prompted the Government of Romania to publish new casualty reduction targets.

Many of the other EU members are aiming for similar reductions. To achieve such targets, the European Experimental Vehicles Committee (EEVC) has recommended a number of 'test methods to evaluate pedestrian protection afforded by passenger cars' (EEVC Working Group, 1998).

The field of road traffic accidents involving pedestrians has been also approached under various aspects by Brunner (2005), Hartmut et al. (2000), Miedreich (2005), Overkott (2006), Depriester (2005), Masson and Serre (2007). Many models have been used and improved along the years to reconstruct and analyse road traffic accidents, from simple mathematical models, analytical relations (Simms et al., 2004) to more complex models included in specialised software (PC-Crash, 2001).

Pedestrian safety is a globally recognised safety concern. Efforts towards modifying vehicle designs to offer some protection for pedestrians began in the early 1970s (Schuster, 2006). Studies concerning pedestrian injuries at speeds below 40 km/h were also carried out by Pohlak et al. (2007). It is widely accepted that a vehicle's leg impact performance is heavily influenced by the bumper system used (Smith et al., 2002), yet, by analysing the pedestrian, through the present paper the authors attempt to find out to what extent the front end of the vehicle influences the pedestrian kinematics and the head injury degree, as it is well known that these traumas are very often fatal.

The pedestrian multibody model can be a good tool to analyse the movement of the pedestrian regarding its impact kinematics and dynamics. For the validation of these models, several crash tests have been performed and will be done. A good correlation between crash tests and simulation results could be found. Different typical shapes of the front hood of modern cars have been used for these crash tests in order to study the influence on the movement of the pedestrian during and after the impact. The model also involves the capability to deal with different kinds of pedestrians (size and mass) under various initial conditions (standing, walking and running) (Moser et al., 2000).

The novel approach taken in this paper consists in studying the contact phase of the impact between the multibody dummy and the vehicle made up of contact bodies whose geometry modifies according to the vehicle profile, with a view to determining the dependency between the injury degree and the vehicle's front-end design.

2 Bumper generalities

An important role in diminishing the frontal or rear impact is held by the elastic and highly resistant structures of bumpers which, together with the side members, partially absorb the impact force. Commonly, all the crash load cases can be defined as low-speed collisions. The bumper was used to reduce the damages resulted from collision at speed below 16 kph (see Ojalvo et al., 1998; Jonsén et al., 2009). In time, the degree of protection assured by the cross member was decreased on the scale of importance, the aesthetic and aerodynamic aspect of the motor vehicle turning out to be more important. Then, it was noticed that the rigidity of the bumper structure or its support elements represent the main element for pedestrians' protection, the deformation being produced in a particular manner which should reduce the impact force upon pedestrians.

The bumper system includes a support and consolidation structure of a curved beam type (there is also the consolidation element which distinct from the bumper), two shock absorbing fixing elements and an elastic mask (fascia) obtained by injection of hard thermoplastic masses made of polycarbonate, polyurethane, polyethylene, polypropylene of high density, thermoplastic rubber or other materials with similar properties.

The bumper is part of a system which includes shock absorbers on which the bumper is fixed, frontal frames and consolidation and fixing elements of the radiator, as well as the headlight system whose protection must be assured.

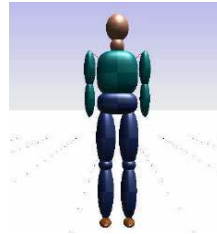
Some research has demonstrated that an adaptive bumper, based on an anisotropic material, could contribute significantly to the 'pedestrian friendliness' of a vehicle's front

end, while retaining high levels of durability. However, before such a concept is ready for full size trials, development of the necessary mechanics is required (Smith et al., 2002).

3 The multibody model

Motor vehicles are generally regarded as rigid bodies for the simulation of traffic accident collisions with kinetic 3D simulation programmes. For collisions with pedestrians, occupants or small objects with multiple components, this simplification does not allow the motion to be accurately modelled. In order to obtain realistic results it is necessary to model pedestrians and many other objects as multibody systems (Moser et al., 1999).

Figure 1 The pedestrian multibody model (see online version for colours)



With the use of multibody systems it is also possible to correlate pedestrian injuries to vehicle damage areas. The multibody pedestrian body elements (head, torso, pelvis, etc.) are interconnected with pivoting joints. For each body there are different properties such as geometry, mass, contact stiffness and coefficients of friction. A general ellipsoid of degree 'n' specifies the geometry for each body (Moser et al., 2000).

4 Vehicle classification upon the front-end design

The motor vehicle's frontal profile is determined, from geometrical point of view, by a series of parameters. Modifying these parameters dictates the framing of specific classes of motor vehicles within geometrical corridors. Likewise, these parameters influence the impact dynamics with the other participants in traffic, such as pedestrians or cyclists.

For some vehicle geometrical parameters identification, that influences the pedestrian's impact, it is presented in Figure 2 the vehicle general profile that includes elements with variable parameters. However, the current vehicle design has evolved comparing to the presented figure, and for these cases some of the presented parameters will have particular values.

Figure 2 Variable geometry vehicle (VGV) schema

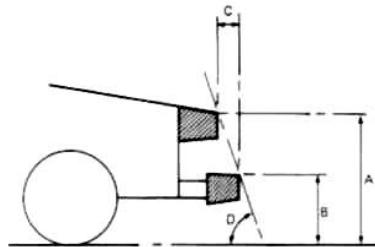


Table 1 Parameters defining the motor vehicle's front end design

<i>Symbol</i>	<i>Name</i>
A	Height of bonnet front edge
B	Height of the bumper upper edge
C	Front edge advance of bumper
D	Angle determined by the bumper upper edge and the bonnet front edge
E	Bonnet inclination angle

First classification version (Dettinger, 1997), accomplished following some DEKRA researches for EEVC-WG17 working group, contains the most usual six vehicle frontal profiles. Geometrical parameters are presented in Table 2.

The geometrical parameters used for profile selection are:

- height of bonnet front edge (distance from the ground)
- bonnet inclination angle (regarding to the horizontal line)
- previous bonnet reference line inclination angle.

Table 2 Initial proposal regarding the geometric frontal profile accomplishment

	<i>Height of bonnet front edge [m]</i>	<i>Bonnet inclination angle [°]</i>	<i>Angle determined by the bumper upper edge and the bonnet front edge [°]</i>
Key profile	< 0.7	< 20	
Trapezoidal profile			
Superficial bonnet inclination		< 20	< 70
Pronounced bonnet inclination		< 20	< 70
Ellipsoidal profile	Bonnet front edge have a radius of curvature > 0.25 m		
Pontoon profile			< 70
Vertical profile (BOX)	Vertically contact plan		

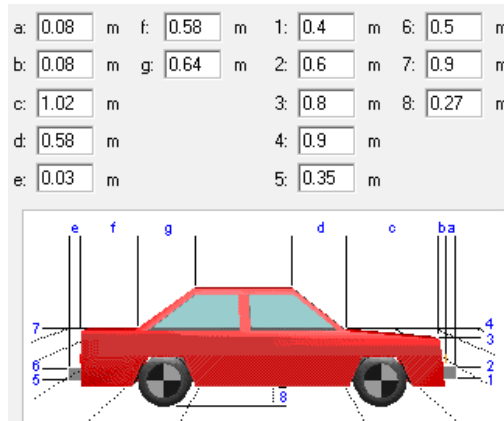
Using PC-crash application there were modified vehicle's frontal geometry parameters with shock absorbent bumper advance variation and through bumper assemblage height variation.

Through modifying these parameters that define the frontal vehicle geometry several vehicle profiles can be obtained, in function of anterior classification. Vehicle geometrical parameters sample is shown in Figure 3 and correspondence between PC-Crash and VGV is shown in Table 3.

Table 3 Correspondence between PC-crash and VGV (variable geometry vehicle)

<i>No. Param</i>	<i>PC-Crash/vehicle's profile</i>	<i>Variable geometry vehicle</i>	<i>Parameter description</i>
P1	1		Height of the bumper lower edge
P2	2	B	Height of the bumper upper edge
P3	3	A	A Height of the bonnet front edge
P4	4		Height of the bonnet rear edge
P5	a	C	Bumper width (bumper advance)
P6	b		Front edge advance of bonnet

Figure 3 Vehicle geometrical parameters sample (see online version for colours)

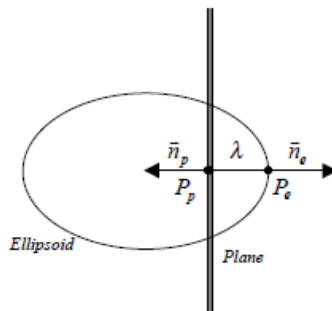


5 Model of the motor vehicle–pedestrian impact

The geometry of the vehicle can have a large effect on the pedestrian dynamics, so the model allows the use of different vehicles shapes. The vehicle shape can be either specified using the menu item, or a detailed 3D DXF shape can be imported and attached to the vehicle (PC-Crash, 2001).

The vehicles in PC-Crash are modelled as a rigid body. The surface of the vehicle is defined by several planes, which are defined by triangular polygons. The vehicle shape can be specified either by entering specific geometrical distances to describe the vehicle shape or by using detailed 3D vehicle shapes imported as DXF drawings. The assumption is made that the point of contact is on the surface of the vehicle plane. Thus, vehicle deformation is neglected. The point of contact has to be inside the three points that define the vehicle’s triangular polygonal plane being contacted. The penetration of the ellipsoid is the distance between a point on the ellipsoid where the tangential plane is parallel to the contacting plane, and the contacting plane. The tangential components of the contact force are calculated using the specified ellipsoid to vehicle friction coefficient and the relative velocity of the contact points. The contact force from the ellipsoid is applied as an external force to the vehicle. Therefore, the influence of a pedestrian impact on the vehicle’s post-impact motion can be analysed (PC-Crash, 2001).

Figure 4 Description of contact between car and human body

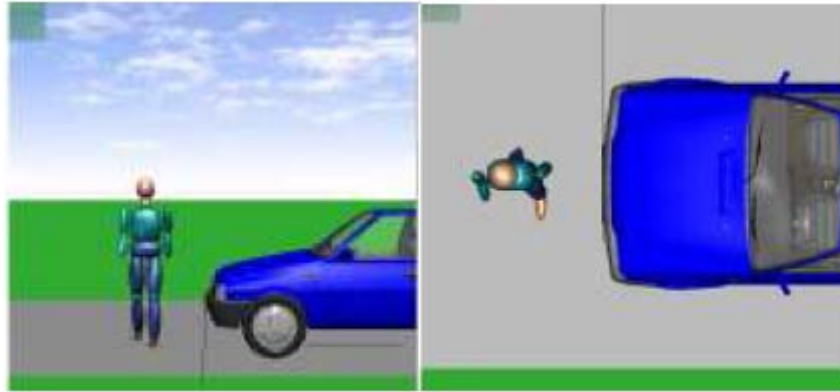


The vehicle submitted to simulations, having a mass of 1100 kg, had some parameters of the front-end geometry modified in accordance with the classification presented Table 2. Vehicle mass was established according to the data, in line with the average mass of European supermini-small family car class.

The simulations undertook vehicle speeds of 30 km/h and, respectively, different stance for the pedestrian. The 30 km/h testing speed was chosen taking into account the technical conditions under which the experimental tests were carried out and which did not allow for higher speeds. The impact between the vehicle and the pedestrian occurred along the longitudinal median axis of the vehicle.

The pedestrian was positioned on the median-right front side of the motor vehicle, having the direction of travel perpendicular to the road axis, the impact occurring on his/her left or right side depending on situation, Figure 5.

Figure 5 Sample test pedestrian initial position (see online version for colours)



The simulations undertook variations of the 'P5' bumper advance, described by the front upper edge, the assembling height of the 'P2' bumper, also measured at its upper front edge and the height of the 'P3' bonnet front edge. The difference between the 'P2' – 'P1' parameters remained constant throughout the tests.

The bonnet inclination angles and the angle determined by the bumper upper edge and the bonnet front edge, 'D' parameter as illustrated in Figure 3, were calculated according to the vehicle profile synthesising shown in Table 2.

$$D = a \tan\left(\frac{P3 - P2}{P5}\right) \quad (1)$$

The simulations led to the determination of impact accelerations and speeds of the pedestrian's head with the vehicle. The accelerations curves enabled the subsequent determination of the head injury criterion HIC, these values being synthesised in a table similar to Table 4. The HIC is the maximum value over the critical time period t_1-t_2 for the expression. The HIC criteria were shown according to the values of 'D' angle.

$$HIC = \max_{t_1, t_2} \left\{ (t_2 - t_1) \cdot \left[\frac{1}{t_2 - t_1} \int_{t_1}^{t_2} a(t) dt \right]^{2.5} \right\} \quad (2)$$

Table 4 Synthesising the data related to the simulations carried out to determine the HIC criterion

		<i>Height of bonnet front edge 'A' = 'P3' [mm]</i>							
<i>Height of the bumper upper edge 'B' = 'P2'</i>	<i>Bumper advance 'C' = 'P5' [mm]</i>								
	30	40	50	60	70	80	90	100	
450	O	O	O	O	O	O	O	O	O
500	O	O	O	O	O	O	O	O	O
550	O	O	O	O	O	O	O	O	O
600	O	O	O	O	O	O	O	O	O

The method used to analyse the data stemmed from simulations was structured throughout the following stages:

- Carrying out an overall analysis of accelerations during the specific time interval;
- Determining time sub-intervals of high interest. These are characterised by the head acceleration values;
- Determining the values regarding the injury criteria;
- Carrying out a comparative analysis of these values in order to determine the influence of front-end design parameters upon the impact with the pedestrian as well as the injury degree.

6 Results and discussion

For the impact speed of 30 km/h, the time taken to head-vehicle's bonnet contact to occur ranges from 0.15 to 0.245 s, being noticed a slight decreasing tendency for a bonnet front edge height of 900 mm, Figures 6–8.

Figure 6 Simulated pedestrian head acceleration for 700 mm bonnet leading edge height (see online version for colours)

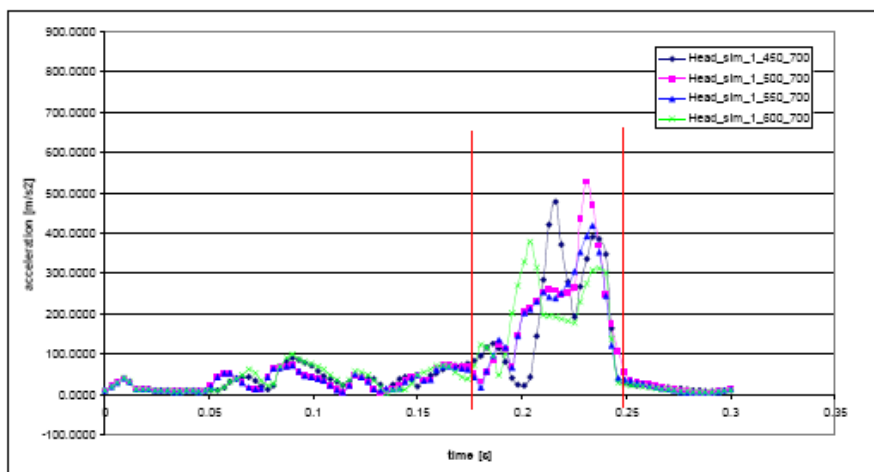


Figure 7 Simulated pedestrian head acceleration for 800 mm bonnet leading edge height (see online version for colours)

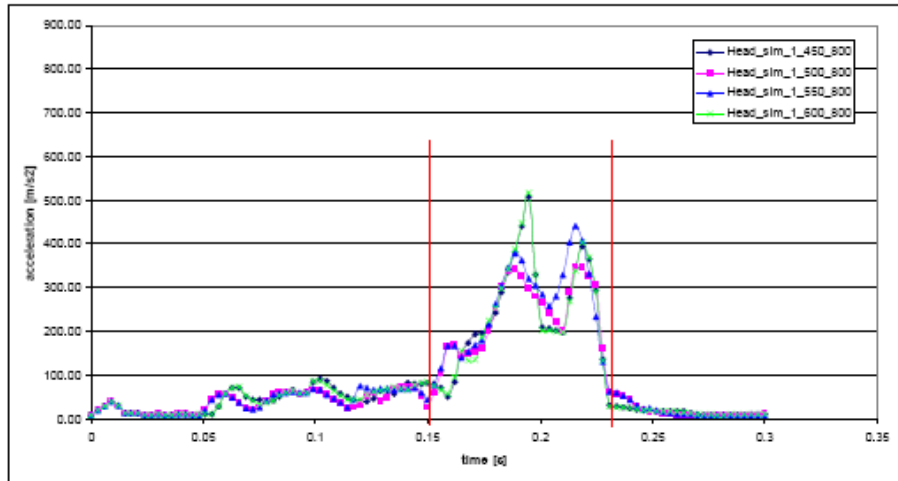
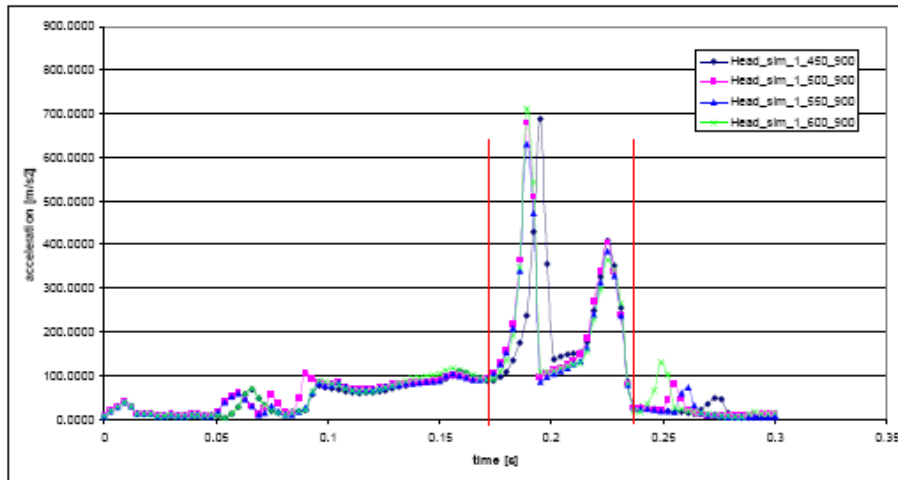


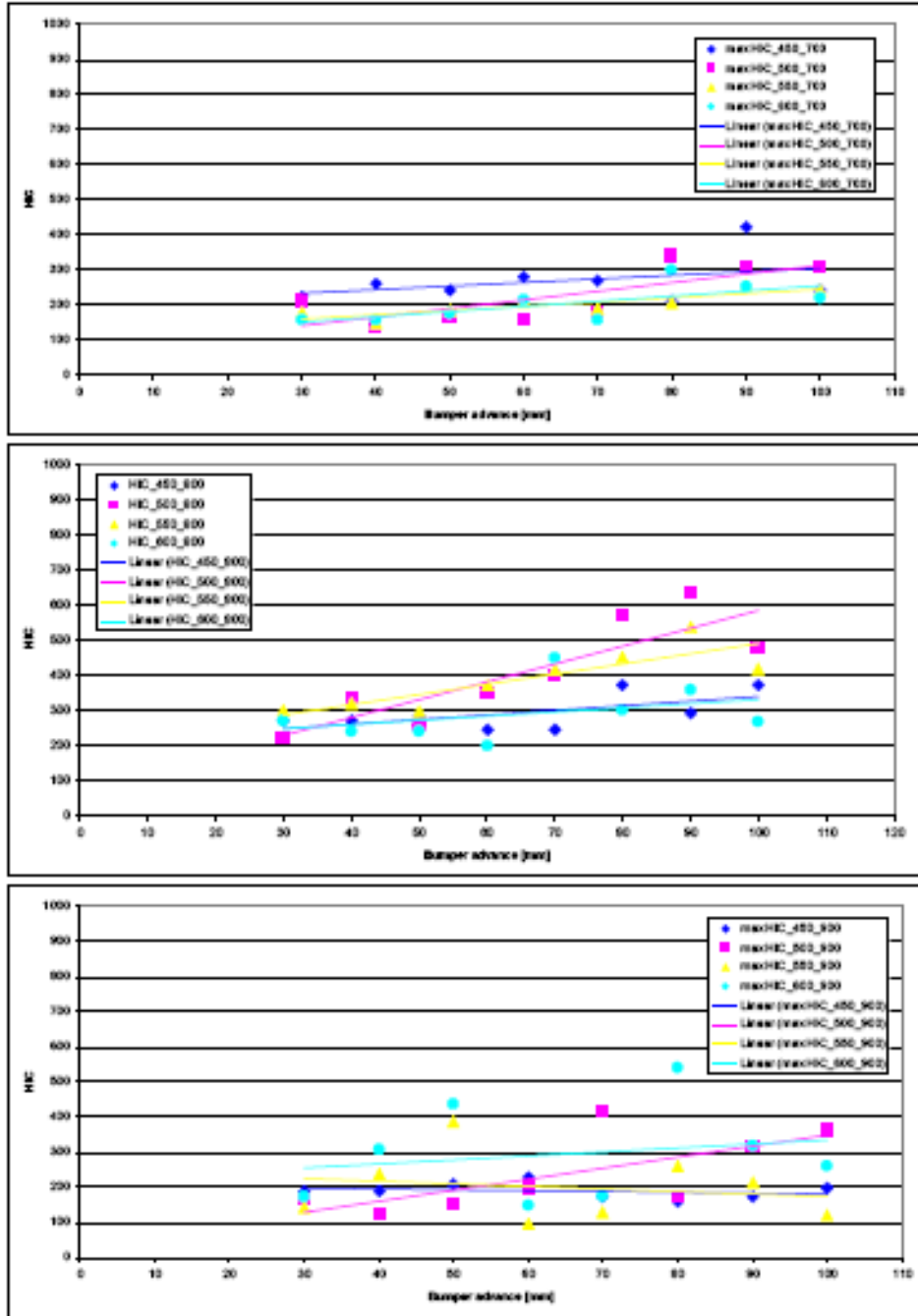
Figure 8 Simulated pedestrian head acceleration for 900 mm bonnet leading edge height (see online version for colours)



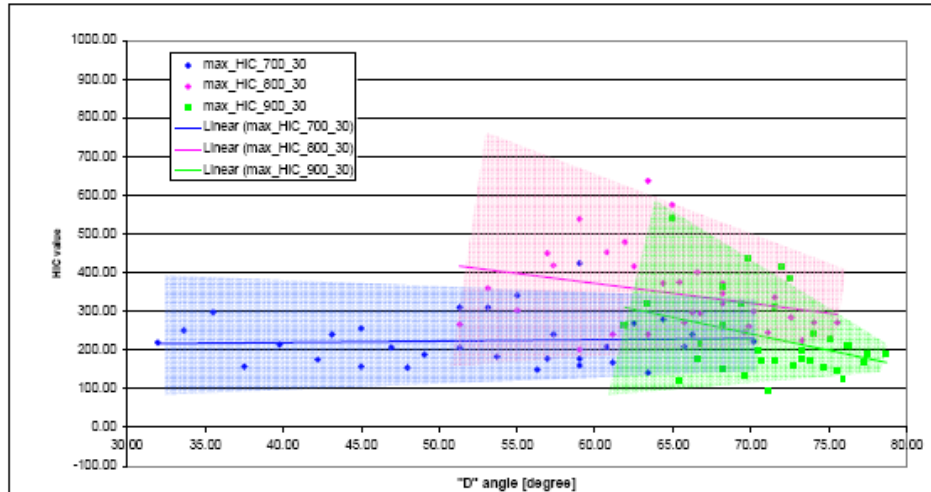
The greater the height of the bonnet front edge is, the higher the head accelerations are, Figure 6–8. The maximum acceleration obtained increases together with the height of the bonnet front edge, reaching a value of 72 G.

With bumper advance variation, parameter ‘P5’, appear an HIC increment following the advance increment, one exception being the almost constant values of the configuration in which the bonnet front edge is situated at 900 mm and the bumper upper edge is at 450 and 550 mm to ground, Figure 9. The HIC variation considering the ‘P2’, ‘P3’ and ‘P5’ parameters shows that the solution to mount the bumper at 600 mm presents a greater dispersion of HIC values than in the other cases, for all the heights of the bonnet front edge chosen in the study.

Figure 9 HIC variation in function of P2, P3 and P5 parameters (see online version for colours)



By representing the HIC value according to angle ‘D’ we notice that the injury level tends to increase with the ‘D’ angle decreasing, an almost constant HIC tendency values occurring in case of the bonnet front edge at 700 mm, Figure 10.

Figure 10 HIC variation in function of 'D' angle (see online version for colours)

The dispersion of HIC values around the regression curves defining the variation tendency presents the greatest variety in case of the configuration with bonnet front edge at 800 mm.

The lower average HIC values for the configuration of the bonnet front edge at 900 mm, as compared to the configuration at 800 mm is explained through the diminishing of the time interval when the impact between the pedestrian's head and the vehicle occurs.

7 Experimental study on the motor vehicle–pedestrian impact

7.1 Testing scenario

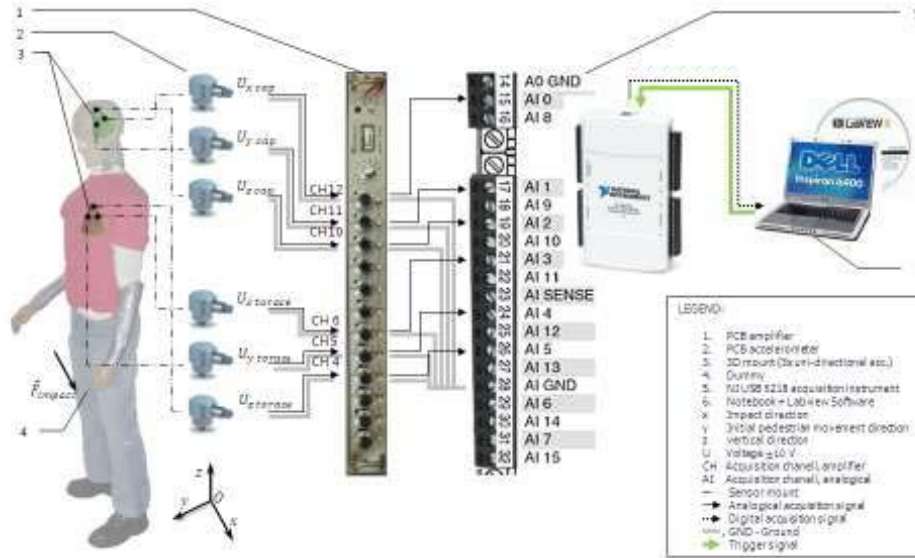
In order to define the tests, a particular situation was considered as representative:

- Pedestrian crossing the street – standing, walking or running – was impacted on its left/right side or both feet, depending by test. A lateral impact was chosen because this position is representative of real accidents as a majority of pedestrians are struck laterally by a vehicle, this type of collision was also being dealt with by Masson and Serre (2007) The both feet of the dummy are in contact with the ground and support the body's weight. The width between both feet was chosen to have a stable stance as the dummy was not sustained by a special harness.
- The motor vehicle runs at a constant speed before the moment of impact.
- The tests were filmed at 125 and 250 shots per second, with natural light.

7.2 Preparing the dummy

In order to meet the construction standards of Hybrid III dummies (FMVSS 572, 1986), the dummy designed and constructed for this type of tests within the Laboratories of the Department of Vehicles and Engines was instrumented with six mono-axial accelerometers mounted on two tri-axial systems on both head and thorax, Figure 11.

Figure 11 Diagram of the measurement chain for data acquisition from sensors applied to the dummy (see online version for colours)



The following operations were carried out:

- Modifying the masses of the dummy's component parts through testing according to Table 5.
- Regulating the moments of friction in joints.

Table 5 Calibrating the dummy's masses

Body segment	Mass after [kg]	obtained calibration
Head	4.50	6.05
Neck	1.55	
Upper and lower thorax	29.65	37.95
Forearms	4.00	
Arms and palms	4.30	
Torso	11.55	29.00
Hip	9.05	
Calf and foot	8.40	73.00
Total weight	73.00	

Particular marks were applied on the dummy, these marks being required for the photo-video analysis of the movement of the various parts of the body.

The measurement chain made up of the previously described equipment is schematically represented in Figure 11.

7.3 *Preparing the motor vehicles*

The vehicles were prepared for tests as follows:

- The fuel tank was empty for safety reasons;
- During the tests, the 5th wheel device was mounted to determine the vehicle speed;
- The frontal surface of the car body was painted in different colours to mark the areas with different potential injury degrees for the pedestrian;
- The surfaces were marked with linear grid and the rims were marked in order to facilitate the image and film analysis;
- The Datalogger OMEGA SHOCK101 and the DSD Pocket DAQ device were mounted according to the axes of the general orthogonal reference system chosen.

7.4 *Experiment development*

The pedestrian was placed in front of the motor vehicle, the position of standing/walking and running. Researchers carry out the tests on two vehicles with different front-end profiles. The speed recorded during the impact was of about 29 km/h for all the three tests, similar to the speeds at which most accidents involving pedestrians and vehicles occur (Nahum and Melvin, 1996). The first vehicle had the bonnet front edge configured at 800 mm to ground; this vehicle was used for tests 1 and 2. The second vehicle had the bonnet front edge configured at 710 mm to ground.

The first impact occurred at tibia level, just under the knee. The vehicle's speed at the moment of impact was around 29 km/h, the motor vehicle hitting the pedestrian in the median area of the bumper. The diagrams analysis shows that for impact speeds of 29.18 km/h, test 1, the duration of the vehicle/pedestrian primary collision is 210 ms, in accordance with the time interval determined following the simulations. For the test 2, this time was 195 ms and at test 3 the time was 200 ms.

The pedestrian hits the vehicle's hood-windshield area with the head. The first lower limb that came in contact with the vehicle was fractured in the region of the knee joint. The experiment shows that the damages caused by the pedestrian occur mainly at windshield level. There were noticed only some traces on the bonnet. The front edge of the bonnet presented a slight imprint of the hip and the upper part of the thigh.

The analysis of data, diagrams and photo-video recordings shows the three typical phases of a motor vehicle-pedestrian impact:

- Phase 1: The contact with the motor vehicle, which lasts from the moment of impact until the moment the pedestrian falls down.
- Phase 2: Throwing phase, which lasts from the moment that pedestrian is thrown until his contact with the ground.
- Phase 3: The contact with the ground, which lasts from the moment that pedestrian reaches the soil until the final position.

The present paper focuses solely on the pedestrian-vehicle contact phase and; therefore, this is the only aspect of the impact submitted to analysis.

7.5 *Contact with the motor vehicle*

The contact between the vehicle and pedestrian walking or running is graphically detailed in Figure 12. First contact is at the passenger knee. It was observed that in the moment next to the bumper/leg contact appears the stricken point ‘drawing’ under the vehicle phenomenon (see Ruşitoru and Soica, 2006; Soica, 2010). This appears because of the knee articulation break after the impact. After that, the passenger is bearing with the femur on the front edge of bonnet, and the impact will be transferred on the other foot.

Figure 12 Sub-phases of the primary impact at 0, 50, 100, 150 and 200 ms, test 1 – pedestrian walking (see online version for colours)



Following this, the pedestrian is rotated on the bonnet and hits the windshield with the head. The photo-video analysis shows the following sub-phases of the impact dynamics and the pedestrian trajectory.

8 **Conclusions**

The analyses carried out in the proposed research theme show that:

- Both simulations and experimental tests led to the following HIC values as illustrated in Table 6. In Figure 14, the authors mark the values corresponding to the bonnet front edge height.
- The approach to modelling of the vehicle impact by using multibody models for pedestrians shows good correlations with the experimental tests on pedestrian's kinematics and dynamics, Figures 12 and 13.
- A minimisation of the HIC criterion is noticed in all cases for parameters ‘P5’, when the advance of the bumper upper edge advance is small.
- The minimum HIC criterion range within the bounds of constant value 200 in the 450 mm height of the bumper upper edge and 700 mm for bonnet leading edge height.
- The head accelerations level did not exceed 72 G, for 30 km/h impact speed.

Figure 13 Simulation sub-phases of the primary impact at 0, 50, 100, 150 and 200 ms, simulation 1 – pedestrian walking (see online version for colours)

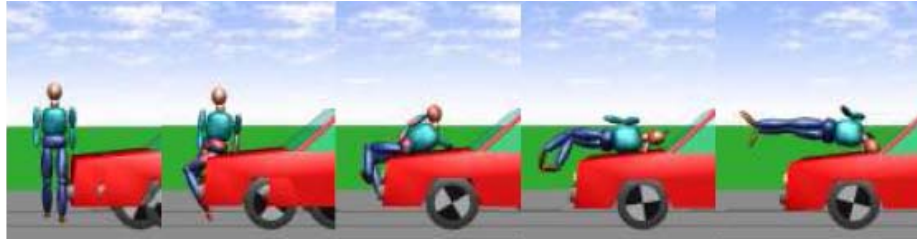


Figure 14 HIC values obtained by test and simulation (see online version for colours)

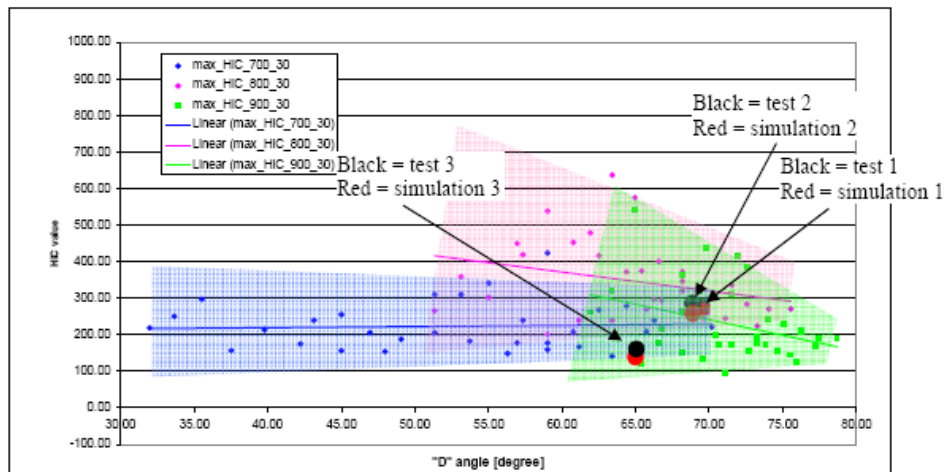


Table 6 HIC values obtained

Item	Simulation	Experiment
1	274	283
2	262	297
3	139	170

References

- Brunner, A. (2005) *Vorlesung: Unfallanalyse und –Rekonstruktion an der FH Konstanz*, DVD.
- Depriester, J.P. (2005) *Comparison of Several Methods for Real Pedestrian Accident Reconstruction*, Criminal Research Institute of the French National Gendarmerie, France.
- Dettinger, J. (1997) 'Beitrag zur Verfeinerung der Rekonstruktion von Fußgängerunfällen', Part.1, Part. 2, *Verkehrsunfall und Fahrzeugtechnik*, 1 January.
- EEVC Working Group (1998) *Improved Test Methods to Evaluate Pedestrian Protection Afforded by Passenger Cars*, European Commission.
- FMVSS 572 (1986) *Subpart E: Hybrid III Test Dummy*, 51 FR 26701 (Standard), 25 July, USA.

- Hartmut, R., Dietmar, O. and Burkhard, S. (2000) 'Pkw-Fussgängerkollisionen im hohen Geschwindigkeitsbereich Ergebnisse von Dummyversuchen mit Kollisionsgeschwindigkeiten zwischen 70 und 90 km/h', *Journal Unfall und Fahrzeugtechnik*, pp.341–346.
- Jonsén, P., Isaksson, E., Sundin, K.G. and Oldenburg, M. (2009) 'Identification of lumped parameter automotive crash models for bumper system development', *International Journal of Crashworthiness*, Vol. 14, No. 6, pp.533–541.
- Kalliske, I. and Friesen, F. (2001) 'Improvements to pedestrian protection as exemplified on a standard-sized car', *2001 ESV Conference*, Paper No. 283.
- Liu, B., Ma, H., Jiang, S. and Du, H. (2009) 'Simulation analysis of human neck injury risk under high-level landing impact', *International Journal of Crashworthiness*, Vol. 14, No. 6, pp.585–590.
- Masson, C. and Serre, T. (2007) *Pedestrian-Vehicle Accident: Analysis of 4 Full Scale Tests with PMHS*, Laboratory of Applied Biomechanics, French National Institute for Transport and Safety Research – Faculty of Medicine of Marseille, Marseille, France.
- Miedreich, M. (2005) 'Fußgängerschutzsystem mit faseroptischen sensor', *ATZ World-wide*, No. 3.
- Moser, A., Hoschopf, H., Steffan, H. and Kasanicky, G. (2000) *Validation of the PC-Crash Pedestrian Model*, SAE 2000 World Congress, SAE Technical Paper 2000-01-0847, Detroit, MI, USA, doi: 10.4271/2000-01-0847.
- Moser, A., Steffan, H. and Kasanicky, G. (1999) *The Pedestrian Model in PC-Crash – The Introduction of a Multi Body System and its Validation*, SAE Technical Paper 1999-01-0445, Accident Reconstruction, Technology and Animation IX, doi: 10.4271/1999-01-0445.
- Nahum, A.M. and Melvin, J.W. (1996) *Accidental Injury*, Springer Verlag, New York.
- Ojalvo, I.U., Weber, B.E. and Evensen, D.A. (1998) *Low Speed Car Impacts with Different Bumper Systems: Correlation of Analytical Model with Tests*, SAE Technical Paper 980365, doi:10.4271/980365.
- Overkott, H., Grohn, R., Görnig, T., Ebner, A. and Roth, G. (2006) "'Intelligenter" Akteur für universelle Fahrzeuganwendungen', *ATZ World-wide*, Nos. 7/8.
- PC-Crash (2001) *A Simulation Program for Vehicle Accidents*, Technical Manual, Version 6.2.
- Pohlak, M., Majak, J. and Eerme, M. (2007) 'Optimization of car frontal protection system', *International Journal for Simulation Multidisciplinary Design Optimization*, Vol. 1, pp.31–37.
- Rusitoru, F. and Soica, A. (2006) 'Aspects regarding the vehicle pedestrian collisions', *The 4th European Academy of Forensic Science Conference*, EAFS2006, Helsinki, Finland.
- Schuster, P. (2006) *Current Trends in Bumper Design for Pedestrian Impact – A Review of Design Concepts from Literature and Patents*, Mechanical Engineering Department California Polytechnic State University, San Luis Obispo, California.
- Simms, C.K., Wood, D.P. and Walsh, D.G. (2004) 'Confidence limits for impact speed estimation from pedestrian projection distance', *International Journal of Crashworthiness*, Vol. 9, No. 2, pp.219–228.
- Smith, A., Ashmead, M., Gay, P. and Siever, N. (2002) *Pedestrian Protection Potential of an Adaptive Bumper*, Cellbond Composites Ltd., Huntingdon, UK.
- Soica, A. (2010) *Siguranta pasivă a autovehiculelor*, Editura Universităţii Transilvania din Braşov, Braşov.
- UNECE (2003) *Child Head Test Method*, INF-GR-PS, 49/IHRA/PS/118R6. Available online at: <http://www.unece.org/fileadmin/DAM/trans/doc/2003/wp29grsp/ps-49.pdf>